

An ADC for the SAM on the SOAR Telescope

Roberto Tighe^{*a}, Andrei Tokovinin^a, Patricio Schurter^a, Manuel Martinez^a, Rolando Cantarutti^a

^aCerro Tololo Inter-American Observatory, Casilla 603, La Serena, Chile.

Abstract

SAM (Soar Adaptive-optics Module), the SOAR (Southern Observatory for Astrophysical Research) GLAO facility is in service since 2011, with a UV, 355nm Laser Guide Star (LGS). The atmospheric wavefront error is therefore measured at 355nm and the star images are corrected in the visible range (BVRI bands). An ADC is required for High Resolution imaging at low telescope elevation, especially at shorter wavelengths of the visible spectrum. The ADC is based on 80mm diameter rotating prisms. This compact unit, fully automated, can be inserted or removed from the tightly constrained SAM collimated beam space-envelope, it adjusts to the parallactic angle and corrects the atmospheric dispersion. Here we present the optical and opto-mechanical design, the control design, the operational strategy and performance results obtained from extensive use in on-sky HR Speckle Imaging.

Keywords: SOAR Telescope, SAM, ADC, Image Quality (IQ), High Resolution Speckle Imaging

Acronyms: GLAO: ground layer adaptive optics, OAP: off-axis parabola, BBAR: broad-band anti-reflective, FP: Fabry-Perot, HR: high resolution, GUI: graphic user interface.

1. INTRODUCTION

The SOAR telescope ¹ has been designed to deliver the highest possible angular resolution at optical wavelengths, thus complementing wide-angle telescopes optimized for surveys and narrow-angle Gemini telescopes specialized for the infra-red. Extending the seeing improvement by fast tip-tilt correction, implemented in the telescope itself with a fast actuated tertiary mirror, to the full adaptive optics (AO) correction is the main purpose of the SAM instrument. It senses the near-ground turbulence with a UV Rayleigh laser guide star and corrects it by a 60-element bimorph deformable mirror (DM). Further information on SAM can be found in Refs. [2,3,4,5].

At optical wavelengths, the atmospheric dispersion (AD), also called chromatic refraction, is a non-negligible contributor to the overall image blur, normally dominated by the seeing. At zenith distance of $z=45^\circ$, the visible spectrum is dispersed by the atmosphere into a 1" line, and this blur rapidly increases as $\tan(z)$ at lower elevations. Even classical seeing-limited instruments require an atmospheric dispersion corrector (ADC). A trombone-type ADC is installed at the optical Nasmyth focus of SOAR ⁶.

SAM needs an ADC even more than other seeing-limited instruments, given that its FWHM resolution can be as good as 0.25" and the relative impact of the (uncorrected) AD becomes correspondingly larger. However, SAM cannot use the trombone ADC because it displaces the optical axis by several arcminutes, and would therefore require a correspondingly large steering of the LGS beam to keep it centered. Instead, the ADC in SAM is installed in the collimated space after the DM, in the science path. It is a classical design with two rotating zero-deviation prisms.

In practice, long-exposure imaging with SAM is often done without the ADC for a number of reasons: pointing errors arising from the fabrication defects of the prisms (see below), observations at long wavelengths and near the zenith where AD remains small, observations in narrow-band filters, and elimination of weak ghosts arising from the ADC prisms. However, when SAM is used with its High-Resolution Camera (HRCam) in the speckle interferometry mode, the AD correction becomes absolutely necessary.

HRCam was initially developed as a simple technical imager for commissioning of SAM. After its first on-sky tests in 2007 ⁷ it became used at SOAR with increasing frequency and produced a substantial number of publications, e.g. Ref. [8]. The total number of speckle measurements done with HRCam at SOAR now exceeds 6000. Over a hundred new binaries were discovered, while orbital motion of many known binaries was followed, leading to the determination or improvement of their orbits.

Speckle interferometry attains the diffraction-limited resolution λ/D , namely 28 mas at 540nm wavelength in the case of SOAR. The AD must be corrected to a fraction of this angle, otherwise the speckle transfer function becomes asymmetric and begins to distort the measurements or to produce false binary discoveries. Before 2010 November, when the ADC was mounted in SAM on-telescope for the first time, HRCam worked without ADC. The effect of AD was

*rtighe@ctio.noao.edu; phone 1 520 318-8000; phone 56 51 2205292; www.ctio.noao.edu

accounted for in the data model ⁹. Needless to say that damping of high spatial frequencies caused by the uncorrected AD reduced the signal to noise ratio and favored the use of narrow-band filters to mitigate its effect, at least partially. In contrast, with the SOAR ADC the AD is no longer an issue, allowing to use wide-band filters such as *I* (788/132 nm) or *V* (550/90 nm), with a substantial gain in sensitivity.

2. OPTICAL DESIGN

2.1 Requirements

In the SAM instrument, the so called “collimated Space” is a cylindrical volume of roughly 135mm long and 100mm in diameter located 45mm after the beam splitting dichroic ^{2,3,4}. This space in which the science beam is parallel, is reserved for an ADC and a tunable Fabry-Perot etalon, Fig 1. The selected FP is an ICOS ET-70, which uses up a length of 75mm leaving an allocated length of about 60mm for the ADC with its supports and mechanisms.

Summary list of requirements:

ADC thickness < 40mm and diameter=80mm

Maximum zenith distance $Z_d \sim 70^\circ$

Wavelengths range 400nm to 800nm

Maximum Field size $3 \times 3 \text{ Arcmin}$

IQ must be diffraction limited for zenith distances up to $Z_d 60$ in the required field and over the wavelength range.

Minimum image displacement with the ADC tracking enabled.

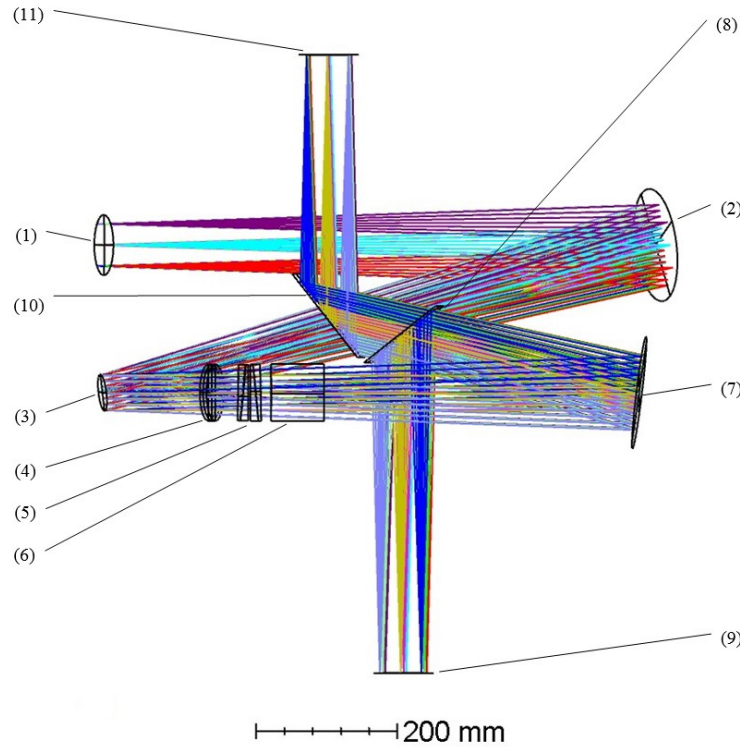


Figure 1. Optical Layout of SAM. (1) SOAR focal plane, (2) OAP 1, (3) DM, (4) Dichroic, (5) ADC, (6) FP, (7) OAP 2, (8) Visitor instrument fold, (9) Visitor instrument focal plane, also HR camera location (10) SAM Imager fold mirror (11) SAMI focal plane.

2.2 Atmospheric Model, in Zemax, for the SOAR Telescope at the Pachón summit

The influence of atmospheric refraction on astronomical observations was reported by G.B. Airy in 1869 together with the idea for correcting the effect ¹⁰, a summary of atmospheric refraction formulas valid for all zenith distances was done

by A.D. Wittmann ¹¹. For Zenith distances from 0 to around 70 degrees, the deviation of the star light due to atmosphere refraction is proportional to $\tan Z_d$ ^{12,13}. If Z_d is the zenith angle of the object star in absence of atmosphere and Z_a the apparent zenith angle of the same object, the refraction of the atmosphere at the entrance of the telescope is given by formula (1).

In practice the difference between Z_d and Z_a at a given wavelength λ_0 is accounted for by a telescope pointing correction and the job of the ADC is to correct the relative dispersion of a given wavelength λ with respect to this wavelength λ_0 .

Atmospheric Refraction in Radians $R = Z_d - Z_a = (n-1)\tan Z_d$ (1)

The Atmospheric Dispersion relative to a given wavelength λ_0 is: $D(\lambda - \lambda_0) = \Delta R(\lambda - \lambda_0) = [n(\lambda) - n(\lambda_0)]\tan Z_d$ (2)

The index of refraction of air depends on wavelength, density, temperature, pressure and composition (mostly dry air, H₂O vapor and CO₂) ¹⁴. The atmosphere above the SOAR telescope on Cerro Pachón was modeled in Zemax using the atmospheric simulation capability of this software. A sanity check of zemax simulation was done using the air index of refraction versus wavelength data from Kitt Peak. Inputting the H and C wavelengths (486.1 and 656.3nm respectively) the Zemax model gave the same result as that published by Breckinridge and McAlister ¹².

The relevant parameters for Atmospheric Simulation at the SOAR site were obtained from the Pachón weather data.

Latitude = 30.238°

Altitude = 2738m above sea level

Temperature = 283K

Pressure = 737mb

Humidity = 0.36 (36%)

The atmospheric dispersion at the SOAR focal plane is given in Table1.

Δy at SOAR focal plane for Z=70Deg	
<u>λ um</u>	<u>Δy mm</u>
0.400	-0.854
0.500	-0.336
0.633	0.000
0.700	0.100
0.800	0.205

Table 1. SOAR focal plane Relative Image displacement, w/r to that at 632.8nm, as a function of wavelength.

2.3 The Prism Design

As explained in the introduction the SOAR trombone type ADC installed in the elevation axis of the telescope, is not appropriate for correcting dispersion in SAM. The general direct vision prism shown made of a two glass combination is the required model. One such prism should compensate half the atmospheric dispersion at Z=70Deg for wavelengths in the range 400-800nm with zero deviation at ~633nm. A pair of rotating identical prisms would compensate for all zenith angles Z < 70Deg and can be oriented parallel to the atmospheric dispersion direction. The glass selection for our starting model was obtained from C.G. Wynne and S.P. Worswick, Ref [15], p.667, Fig.6.

The formulas to calculate the apex angles A_1 and A_2 for our starting model, valid for small angles ¹⁶ are:

$$A_1 = dD_{12} V_1 V_2 / (n_1 - 1) (V_2 - V_1) \quad (3)$$

$$A_2 = dD_{12} V_1 V_2 / (n_2 - 1) (V_1 - V_2) \quad (4)$$

Where dD_{12} is the angular dispersion difference in radians between λ_1 and λ_2 to be produced by the prism, n_1 and n_2 are the indices of refraction of glasses 1 and 2 and V_1 and V_2 the Abbe numbers of glasses 1 and 2.

The inner surfaces of the two prisms need to be perpendicular to the axis to allow for rotation, so the tilt of these surfaces is zero.

The ADC prisms are mounted in the Zemax SOAR model with telescope at zenith, i.e. Z=0Deg. Optimization consists of reproducing at the SAM focal plane, the same dispersion the atmosphere would produce at the SOAR focal plane with the telescope at zenith value of 70Deg.

The main Zemax operands to do this are:

REAY, set a target value of the Y position of the image at each wavelength, equal to the respective values in Table1.

CENX and CENY, set both equal to zero for the central wavelength of 0.6328um.

MNCT and MXCT, set values to constrain the glass thicknesses (6mm< CT <8mm).

Then select plausible glass pairs and set variables on prisms surfaces tilts and on glasses thicknesses.

The best results for our case were obtained by a combination of BaK2 and CaF2 glasses. The details of the optimized ADC for SAM are shown in Fig 2.

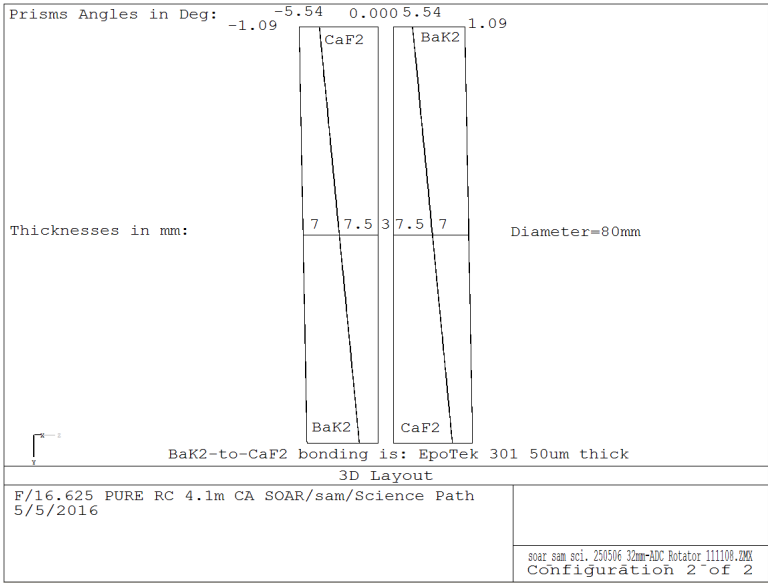


Figure 2. The optimized SAM ADC dimensions for fabrication.

Optical manufactures were reluctant to fabricate 80mm diameter prisms with less than ~6mm central thickness. Shallow tilt angles of less than ~1deg also pose difficulties in meeting tight specs for manufacturing. These identical prisms shown in Fig 2, were manufactured for us by RMI (Rocky Mountain Instrument Company). The glass to air surfaces were coated with a BBAR coating with a Reflectance at normal incidence of ~0.5 % from 400 to 900nm.

2.4 Optical performance

The residual dispersion at the design zenith angle of 70Deg is shown in Fig 3 and the prisms angular position for best correction as a function of zenithal distance, as given by the Zemax model, is shown in Fig 4.

Uncorrected and Corrected dispersion at Z=70Deg		
λ μm	Uncorrect. Δy mm	corrected Δy mm
0.4000	-0.8540	0.0034
0.5000	-0.3360	0.0044
0.6328	0.0000	0.0084
0.7000	0.1000	0.0044
0.8000	0.2050	-0.0086

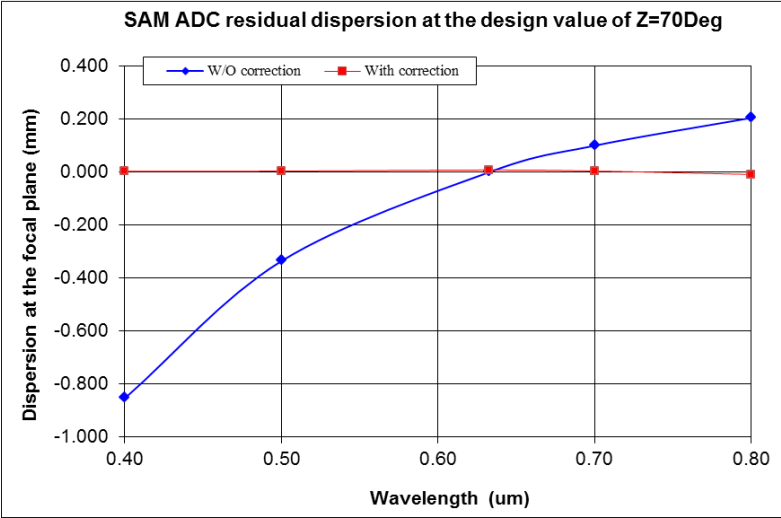


Figure 3. SAM focal plane residual dispersion from 400 to 800nm, before and after correction. The plot data at the right.

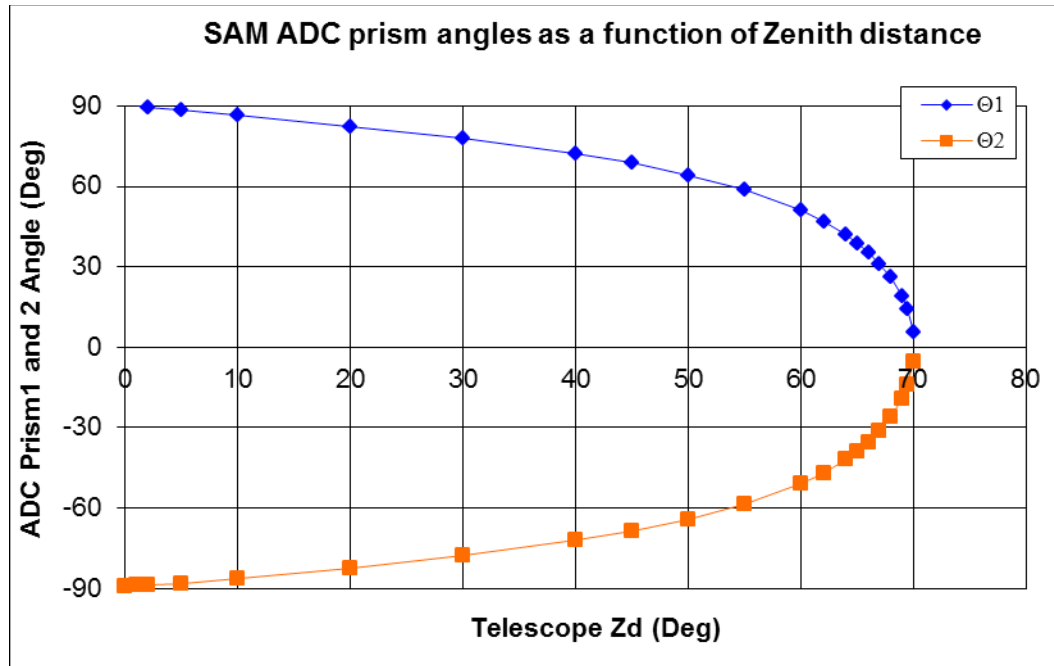


Figure 4. SAM ADC prism angles vs Zenith distance

The atmospheric dispersion corrected spot diagram at the SAM focal plane for a SOAR telescope zenith distance of 60Deg is shown in Fig 5.

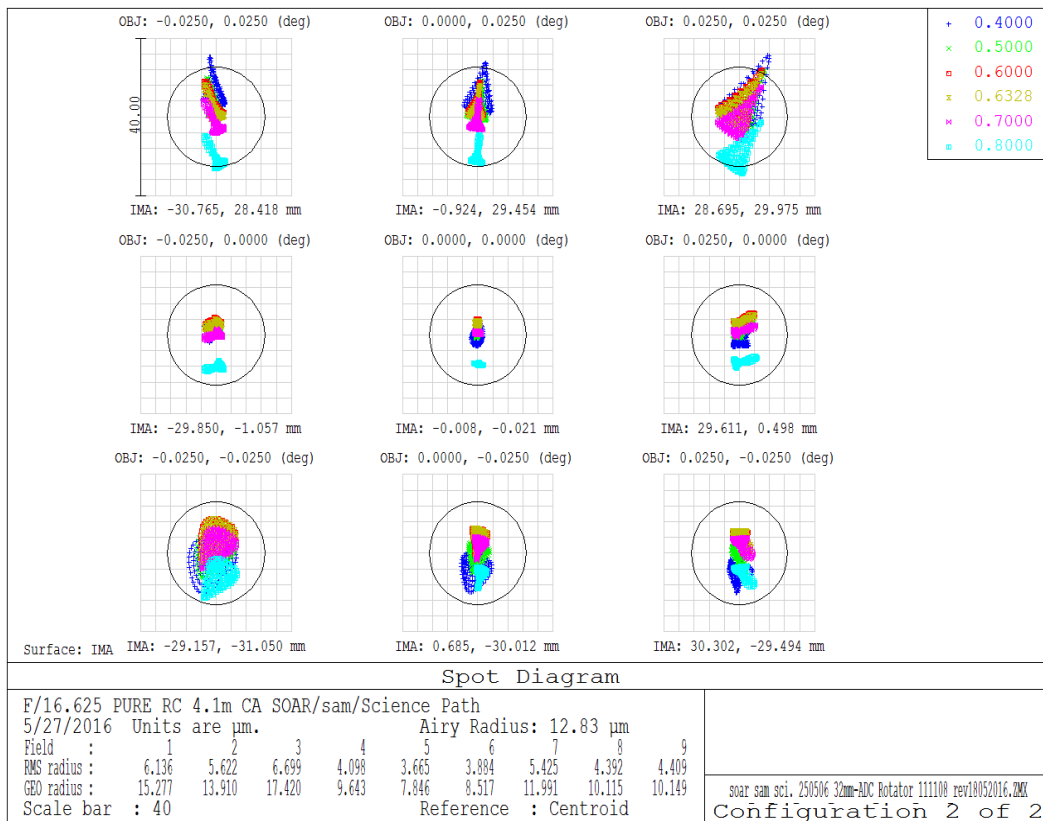


Figure 5. SAM 3'x3' field atmospheric corrected dispersion spot diagram for Z=60Deg.

3. OPTO-MECHANICAL DESIGN

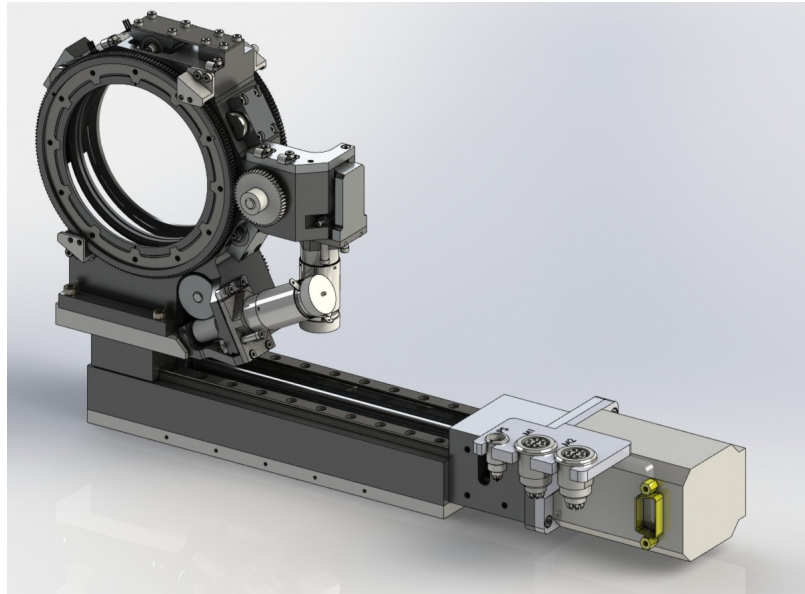


Figure 6. Overall view of the ADC

The ADC module of SAM was designed to be remotely deployed into the collimated space of SAM. The available space for this mechanism is a volume of approximately 60 x 210 x 330 mm, where 60mm is the distance along the optical path.

The overall width of the ADC is less than 50mm, making it very compact. The distance between the prisms is 4.6mm.

To provide insertion and removal of the ADC system, the ADC is mounted on a Dover Motion (Previously Danaher) KV-140 linear stage driven by a Quicksilver QCI-A17 smart motor. The stage has 140mm of travel and is repeatable to $\sim 3\mu\text{m}$ according to its manufacturer.

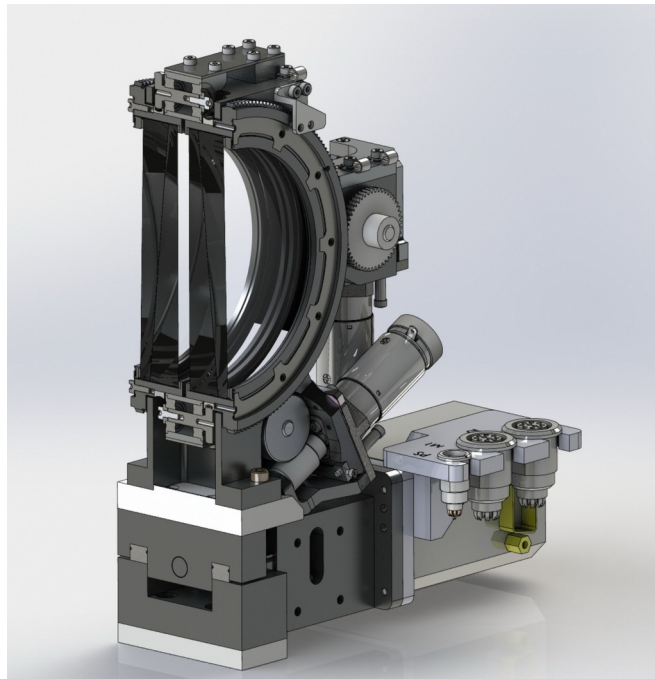


Figure 7. A cut view of the ADC

Each prism is held in its cell with the aid of a machined wedge that matches the angle on each prism to provide parallel faces. Prism and wedge are preloaded by a leaf spring. Each cell has a stainless steel track on its outside with a concave round profile. The cells are registered against three wheels with a matching round profile to provide auto-centration. Two wheels are fixed and the third one is preloaded. In this way, each cell is semi-kinematically mounted to the main housing of the ADC. The position of the fixed wheels was adjusted using shims to assure concentricity of the two prisms.

The prisms cells are rotated independently by means of a 200teeth, 0.5M gear cut into each cell. This gear is in turn driven by a 48 teeth anti-backlash pinion which is attached to a 1:40 worm gear driven by a 4.4:1 geared Maxon DC motor. The worm is preloaded to the gear by means of a leaf spring. The total ratio between the motor and each prism is 730.4:1. A rotational resolution of ~ 3.5 arcsec per step is possible with this system, which complies with the operational requirements for prism rotation. The rotation angle of each prism is calculated by means of step counting after referencing the prisms to a fiducial, the Hall effect sensor in Fig 8. Since there is no contact between the cell and the mechanism's housing, each cell can rotate freely without possibility of collision.

4. ADC CONTROL, ELECTRONICS AND SOFTWARE

4.1 Electronics

The motors for prism rotation are Maxon^{MR} model 215 996 with the reduction box model 110321. The angular position is given by an incremental encoder, model 201940, on the motor shaft. Two position control servo boards AllMotion^{MR} EZSV23 are used, one for each prism as shown in Figure 8.

The motor-gearbox combination plus the gear drive mechanism provides a maximum speed of 6.86 rpm. The incremental encoder is 512 counts per turn with differential output.

The ADC unit is inserted or removed from the optical path using a Danaher^{MR} model KV-140 (NEMA 17) linear stage driven by a QuickSilver^{MR} motor model QCI-A17H-1-A01. Movement control provides IN and OUT positions defined by centering in the optical beam and out of the optical beam respectively.

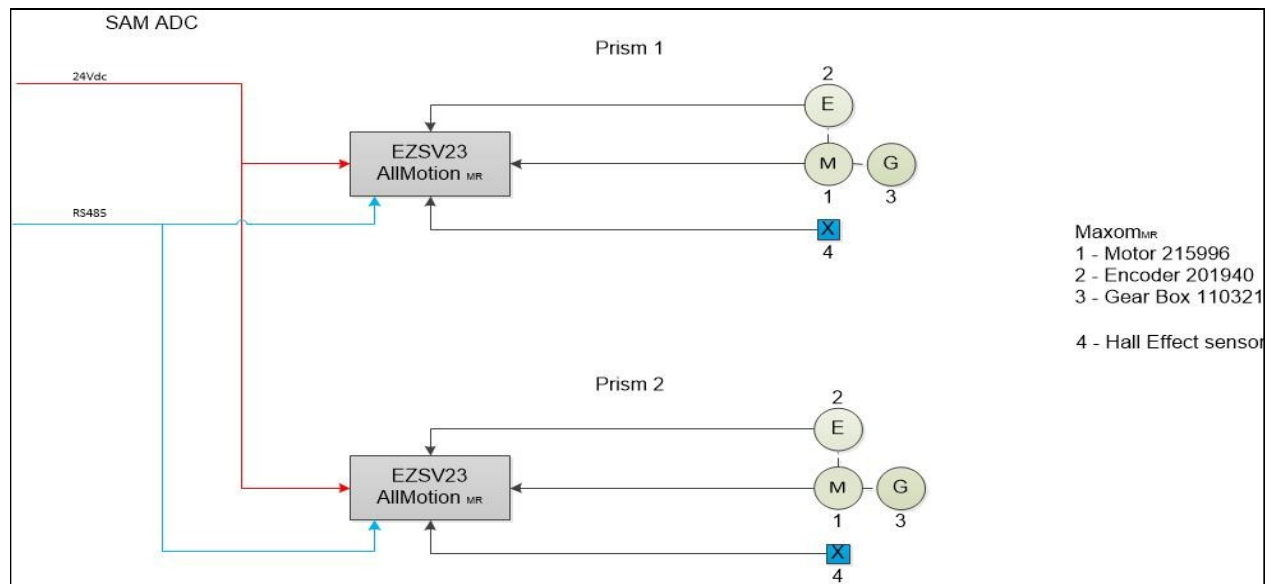


Figure 8. ADC prism motion control

An interface was built to accommodate the differential signal to TTL, which is the signal type accepted by the servo board. For each prism, an Allegro A1205 Hall effect sensor is used for home position reference with a repeatability much better than the acceptable positioning error of the ADC, which is ~ 0.5 Deg. Position control and telemetry for the ADC system is implemented in the Motion Control GUI of the instrument, Fig 9.

The GUI is designed in Labview^{MR}. It provides commands for movement, status and initialization of the prisms. Communication between the motion control graphic interface and the servo boards is via RS485.

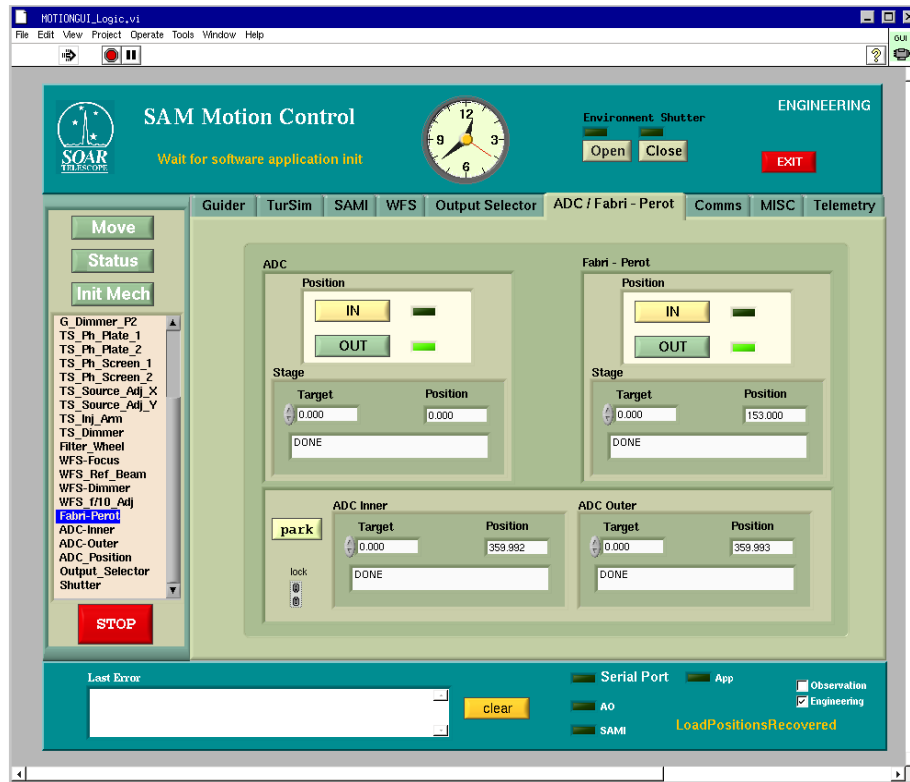


Figure 9. Screenshot of the motion control GUI

4.2 Software

The ADC module is controlled from the instrument computer (IC). The IC is housed in a cabinet on the SOAR mount platform and it hosts four of the five software modules that control the SAM instrument. The IC operates under Linux and all the software modules are written in LabVIEW. The software modules are accessed by VNC connections either from the SOAR console room or remotely.

The linear stage and the two servo boards for the ADC are connected to the serial RS-485 bus of the SAM adaptive-optics module (AOM) and accessed by a communication board in the IC. The AOM motion control software module takes care of the position control and telemetry at a low level, providing interfaces to initialize, move and query status of the ADC mechanisms either locally, through its graphical user interface (GUI), or remotely via sockets.

In normal use, SAM is controlled only through the instrument control software module (ICSOFIT) and there is no need to access the other modules. The ICSOFIT is a high-level LabVIEW application used to operate the whole instrument. It communicates with the lower-level modules and the telescope control system (TCS) through sockets. A dedicated tab control in its GUI contains indicators and controls for automatic operation of the ADC depending on the current telescope elevation. Controls for semi-automatic operation are provided as well.

4.2.1 AOM motion control software module

The AOM motion control module is a multithreaded LabVIEW application comprised of several independent tasks that work cooperatively to provide control over a range of hardware modules including the ADC mechanisms.

Common to all ADC mechanisms, two independent finite-state machines are at the core of their motion control logic. One takes care of the initialization of the mechanism, and the other takes care of moving the mechanism to a specified final position. Typically the initialization state machine jogs the mechanism to find a home limit and updates its encoder counters to a predefined angle value in the 0-360 degrees range. The motion state machine starts by checking i) if the mechanism was initialized and ii) if the final position is within the allowable range. Only then the mechanism is moved to the commanded position.

An independent task polls for status of the ADC mechanisms, including current position and overall health state, and makes the information available locally and remotely.

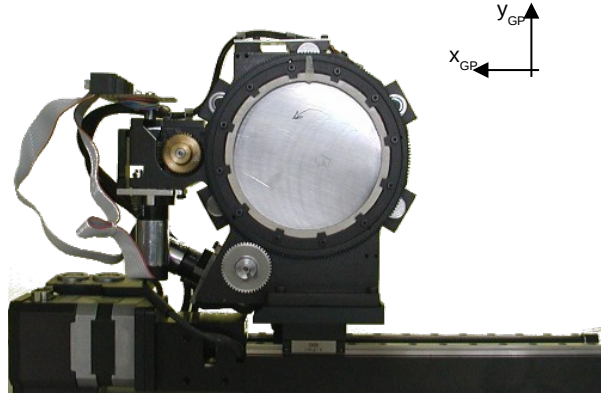


Figure 10. The linear stage and the two servo boards are connected to the serial RS-485 bus of the SAM AOM.

4.2.2 Instrument control software module

The instrument control module is also a multithreaded LabVIEW application. Among several other tasks that comprise the instrument control module application, is the ADC task. The task waits forever in a queue for one of two possible type of commands to arrive. A command with two arguments implies a target position for the prisms. A command with no arguments implies that the prisms positions should be automatically computed based on the current telescope elevation. In both cases the prism angles are routed to the AOM motion control module to perform the actual motion of the ADC mechanisms.

When the automatic ADC compensation is enabled in the ICSOFT, the ADC tasks is prompted to do its job every 5 seconds. The process starts by obtaining the dispersion orientation angle (DA) referenced to the ADC angular coordinates. Then the zenithal distance is used to obtain the angle of the prisms with respect to the DA and compute the final target position for each mechanism. Following is a representation using pseudo code of the main computations involved in the process. The parameter STRENGTH has a typical value of 0.3603.

```

if(STRENGTH * tan(ZD) < 1)
    ANGLE = 90° - asin(STRENGTH * tan(ZD))
else
    ANGLE = 90°
DA = 263° - atan2(cos(ROT - EL), -sin(ROT - EL))

INNER = DA - ANGLE
OUTER = DA + ANGLE

```

(5)
(6)

Where ZD is the zenith angle, DA is the dispersion angle, ROT is the SOAR Nasmyth rotator angle, EL is the telescope elevation angle and INNER and OUTER are the requested angular positions of the ADC prisms.

5. OPERATION AND PERFORMANCE OF THE SAM ADC

Figure 12 shows a slight displacement of the star image in the direction perpendicular to dispersion, under an 85Deg rotation of the prisms. We believe we've traced this defect to a slight mismatch in alignment of the wedge vertices of the two glass components of each prism, during the bonding process. A higher precision orientation control of the prisms components while gluing them would be advisable.

Because of this image shift, in HR imaging the ADC is left to adjust automatically according to the telescope pointing position. But once the prisms arrive in position as determined by (5) and (6), the ADC tracking is disabled during observation of the target.

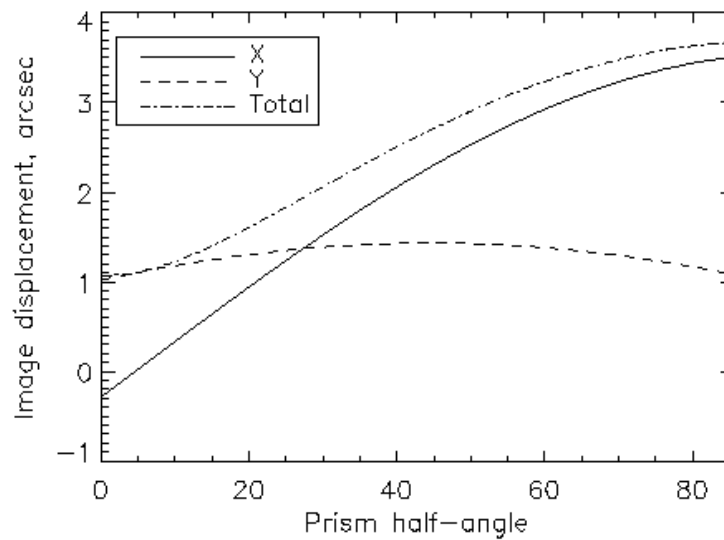


Figure 11. Image shift at SAM focal plane under $\sim 90^\circ$ rotation

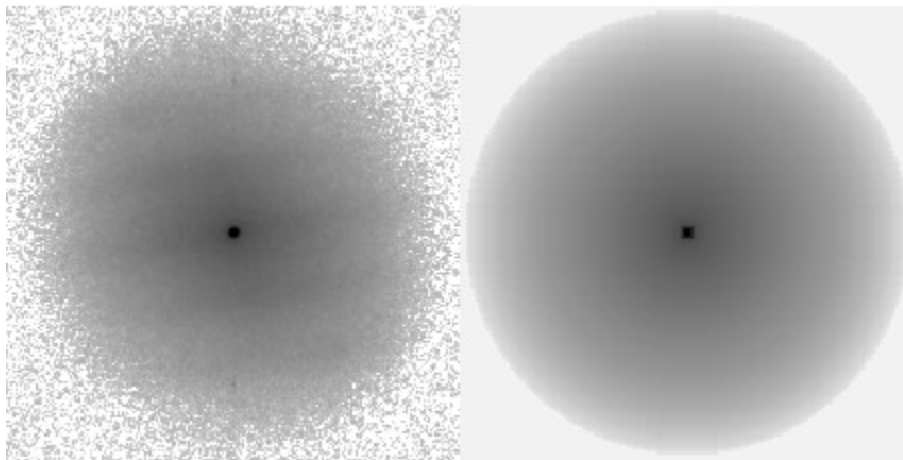


Figure 12. Power spectrum of the single bright star 104 Tau recorded with HRCam on 2016 February 20 at zenith distance of 50.8° in a filter with central wavelength 522 nm and bandwidth 22nm.

The power spectrum in Fig 13 is displayed on the left in the logarithmic scale, its rotationally-symmetric model is shown on the right for comparison. With a pixel scale of 15.2 mas, the image is Nyquist-sampled, and the speckle power is detected up to the cutoff frequency, symmetrically in both coordinates. This attests to the excellent AD correction: without it the image blur would be 7.5 pixels in the vertical direction.

REFERENCES

- [1] Thomas A. Sebring; Gerald N. Cecil; Gilberto Moretto, "SOAR Telescope Project: a four-meter telescope focused on image quality", *Proc. SPIE* 3352
- [2] Tokovinin A., Tighe R., Schurter P., Cantarutti R., van der Blik N., Martinez M., Mondaca E., Montane A., SAM: a facility GLAO instrument, *Proc. SPIE* 7015, Adaptive Optics Systems, 70154C (July 14, 2008).
- [3] Tokovinin A., Tighe R., Schurter P., Cantarutti R., van der Blik N., Martinez M., Mondaca E., Montané A., Naudy W., SAM sees the light, 2010, *SPIE Proc. Vol. 7736*, 132.

- [4] Tokovinin A., Tighe R., Schurter P., Cantarutti R., van der Blik N., Martinez M., Mondaca M., Heathcote S., Performance of the SOAR adaptive module with UV Rayleigh guide star, *Proc. SPIE* 8447, Adaptive Optics Systems III, 84474H (September 13, 2012).
- [5] Tokovinin A. Cantarutti R., Tighe R., Schurter P., Martinez M., Thomas S., van der Blik N., SOAR Adaptive Module (SAM): Seeing Improvement with a UV Laser, Publ. Astron. Soc. Pac.: PASP-100129, 25 May 2016.
- [6] http://www.lna.br/wsnoinstr/ftp/GOODMAN_preparing_for_MOS_guidelines.pdf.
- [7] Tokovinin, A., Cantarutti, R. First speckle-interferometry at SOAR telescope with electron multiplication CCD, *PASP*, 120, 170-177 (2008).
- [8] Tokovinin, A., Mason, B.D., Hartkopf, W.I., Mendez, R.A., Horch, E.P. "Speckle interferometry at SOAR in 2015." *AJ*, accepted (2016)
- [9] Tokovinin A., Mason B.D., Hartkopf W.I. "Speckle interferometry at Blanco and SOAR telescopes in 2008 and 2009" *Astron. J.*, 139, 743-756 (2010).
- [10] George B. Airy, On Atmospheric Chromatic Dispersion as affecting telescopic Observations and on the Mode of correcting it, *Mon. Not. R. Astron. Soc.* 29, 333 (1869).
- [11] Wittmann, A. D., Astronomical refraction: formulas for all zenith distances, *Astronomische Nachrichten*, vol. 318, no. 5, Issue 5, p. 305., 1997AN....318..305W ([SAO/NASA Astrophysics Data System \(ADS\)](#)).
- [12] J.B. Breckinridge H.A. McAlister and W.G. Robinson, Kitt Peak speckle camera, *App. Opt.* vol. 18, No7, 1 April 1979.
- [13] H. Dekker and B. Delabre, Simple wide-band atmospheric dispersion corrector, *Applied Optics* (1987) Vol26, No8, 1375-1376.
- [14] C.J.C. Owens, Optical Refractive Index of Air: Dependence on Pressure, Temperature and Composition, *Applied Optics*, Vol. 6, No. 1, 1967, p.51 – 59.
- [15] .G. Wynne and S.P. Worswick, Atmospheric dispersion corrector at the Cassegrain focus, *Mon. Not. R. Astr. Soc.* (1986) 220, 657-670.
- [16] Warren J. Smith, *Modern Optical Engineering*, McGraw-Hill Inc., 2nd edition 1990, p. 90-91.